A GENERAL ALGORITHM FOR CALCULATING FORCE HISTOGRAMS USING VECTOR DATA

Daniel Recoskie, Tao Xu and Pascal Matsakis
School of Computer Science, University of Guelph, Guelph, Ontario, Canada

Keywords: Relative position descriptors, Shape descriptors, Polygonal objects.

Abstract: The histogram of forces is a generic relative position descriptor with remarkable properties, and it has found many applications, in various domains. So far, however, the applications involve objects in raster form. The fact is that several general algorithms for the computation of force histograms when dealing with such objects have been developed; on the other hand, there is no general algorithm available for objects in vector form, and the algorithms for raster objects cannot be adapted to vector objects. Here, the first general algorithm for calculating force histograms using vector data is presented.

1 INTRODUCTION

The histogram of forces is a generic relative position descriptor with high discriminative power and remarkable properties. It was introduced by Matsakis and Wendling (1999) with the aim of developing new models of directional relations (such as right, left, above, below) between 2-D objects. The spatial organization of 2-D objects is a subject of interest in many disciplines (e.g., computer science, cognitive science, linguistics, geography), with applications in various domains (e.g., medical imaging, robot navigation, content-based image retrieval, geographic information systems). The histogram of forces has been used, e.g., in a geospatial information retrieval and indexing system (Shyu et al., 2007); for scene matching (Sjahputera and Keller, 2007); to interpret human-to-robot commands and generate robot-to-human feedback (Skubic et al., 2004); along with a land cover classification system (Vaduva et al., 2010). Many other applications are mentioned in a recent paper by Matsakis et al. (2011): the classification of skull orbits and sinuses; the recognition of graphical symbols in technical line drawings; the translation of hand-sketched route maps into linguistic descriptions; etc. The above-mentioned applications deal with 2-D objects in raster form. These objects can be crisp or fuzzy, connected or disconnected, with or without holes, disjoint or overlapping. The fact is that several general algorithms for the computation of force histograms when dealing with such objects have been developed. The traditional algorithm (Matsakis and Wendling, 1999) runs in O ($Kk^2N\sqrt{N}$) time, where K is the number of directions in which forces are considered, k is the number of nonzero membership degrees and N is the number of pixels in the image. A variant runs in O ($KkN\sqrt{N}$) time. Another runs in O ($KN\sqrt{N}$) (Wang et al., 2004). A completely different algorithm is in O ($N \log N$) (Ni and Matsakis, 2010). Which algorithm or variant performs better under which conditions is an issue discussed by Ni and Matsakis (2010). As these authors acknowledge, however, the algorithms above cannot be adapted to objects in vector form, and there is no general algorithm for the computation of force histograms in the case of vector objects (Matsakis et al., 2011). The present paper fills this important lacuna. The concept of the histogram of forces is described in Section 2. The new algorithm is introduced in Section 3. Experimental results follow in Section 4, and Section 5 concludes the paper.

2 BACKGROUND

2.1 Objects

Consider a fuzzy subset A of the Euclidean plane. Every point p of the plane has therefore a grade of

Recoskie D., Xu T. and Matsakis P. (2012).
A GENERAL ALGORITHM FOR CALCULATING FORCE HISTOGRAMS USING VECTOR DATA.
In *Proceedings of the 1st International Conference on Pattern Recognition Applications and Methods*, pages 86-92
DOI: 10.5220/0003781600860092

membership in A. This grade, $A(p)$, is 0 if p does not belong to A at all; it is 1 if p totally belongs to A; it is a value between 0 and 1 otherwise, and the greater $A(p)$ the more p belongs to A. The α-cut of A, where $0<\alpha\leq 1$, is the (crisp, ordinary) set of points p such that $A(p)\geq\alpha$. In this paper, an *object* is a fuzzy subset A of the Euclidean plane such that any $A(p)$ belongs to the set $\{\alpha_1,\alpha_2,\ldots,\alpha_{k+1}\}$, with $1=\alpha_1>\alpha_2>\ldots>\alpha_{k+1}=0$, and the intersection between any α_i-cut of A and any straight line has a finite number of connected components.

2.2 Force Histograms

Consider two distinct infinitesimal particles p and q of mass m and n. According to Newton's law of gravity, p exerts on q the force

$$mn\ \overrightarrow{qp} / |\overrightarrow{qp}|^3, \tag{1}$$

where $\overrightarrow{qp}$ is the vector from q to p and $|\overrightarrow{qp}|$ its length. This force tends to move q towards p, and its magnitude is $mn / |\overrightarrow{qp}|^2$. Now, consider two objects A and B. They can be seen as flat metal plates of constant and negligible thickness: the area mass density of A at point p is the grade of membership $A(p)$, and the area mass density of B at q is $B(q)$. Every point p of A exerts on every $q\neq p$ of B an infinitesimal gravitational force, and the vector sum of all these forces, i.e., the resultant force exerted by A on B, can be found using integral calculus. Instead, consider a real number r and a direction θ, replace (1) with (2), or with (3), and calculate the magnitude $\varphi_r^{AB}(\theta)$ of the vector sum of all the infinitesimal forces in direction θ (Fig. 1). The function φ_r^{AB} so defined is called a force histogram. It is one possible representation of the position of A relative to B.

$$mn\ \overrightarrow{qp} / |\overrightarrow{qp}|^{r+1} \tag{2}$$

$$\min\{m, n\}\ \overrightarrow{qp} / |\overrightarrow{qp}|^{r+1} \tag{3}$$

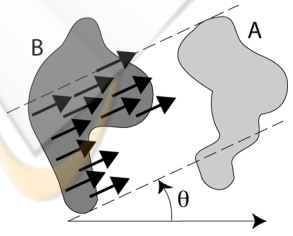

Figure 1: Every point of A exerts on every point of B an infinitesimal force. Using integral calculus, find the vector sum of the forces in direction θ. Its magnitude is $\varphi_r^{AB}(\theta)$.

2.3 Properties

The interest in force histograms lies in the fact that they are relative position descriptors with high discriminative power and remarkable properties.

Consider a real number r and two objects A and B. Equation (4) holds for any θ.

$$\varphi_r^{BA}(\theta) = \varphi_r^{AB}(\theta+\pi) \tag{4}$$

Let *rot* be a ρ-angle rotation and let *sca* be a uniform scaling with positive scale factor λ. The force histograms $\varphi_r^{rot(A)\ rot(B)}$ and $\varphi_r^{sca(A)\ sca(B)}$ can be expressed in terms of φ_r^{AB}. Equations (5) and (6) hold for any θ.

$$\varphi_r^{rot(A)\ rot(B)}(\theta) = \varphi_r^{AB}(\theta-\rho) \tag{5}$$

$$\varphi_r^{sca(A)\ sca(B)}(\theta) = \lambda^{3-r}\varphi_r^{AB}(\theta) \tag{6}$$

Actually, any $\varphi_r^{aff(A)\ aff(B)}$, where *aff* denotes an invertible affine transformation, can be expressed in terms of φ_r^{AB}. See (Matsakis et al., 2011) (Ni and Matsakis, 2010) for details. Note that the grade of membership of a point p in the object *aff*(A) is, by definition, $aff(A)(p)=A(aff^{-1}(p))$; likewise, $aff(B)(p)= B(aff^{-1}(p))$. Now, let A^i denote the α_i-cut of A and let B^j denote the α_j-cut of B. If the forces are as in (2), then (7) holds; and if they are as in (3), then (8) holds.

$$\varphi_r^{AB}(\theta) = \sum_{i=1}^{k}\sum_{j=1}^{k}(\alpha_i-\alpha_{i+1})(\alpha_j-\alpha_{j+1})\,\varphi_r^{A^iB^j}(\theta) \tag{7}$$

$$\varphi_r^{AB}(\theta) = \sum_{i=1}^{k}(\alpha_i-\alpha_{i+1})\,\varphi_r^{A^iB^j}(\theta) \tag{8}$$

Assume A and B are crisp, i.e., all grades of membership are in $\{0,1\}$. Consider a tuple $(A_1, A_2, \ldots, A_a)$ of crisp objects, where a is a positive integer. Assume the interior of $A_i \cap A_j$ is empty for any $i\neq j$ and the closure of A is equal to the closure of $\cup_i A_i$. We then say that $(A_1, A_2, \ldots, A_a)$ is a *partition* of A. Likewise, assume $(B_1, B_2, \ldots, B_b)$ is a partition of B. Equation (9) holds for any θ.

$$\varphi_r^{AB}(\theta) = \sum_{i=1}^{a}\sum_{j=1}^{b}\varphi_r^{A_iB_j}(\theta) \tag{9}$$

r has an interesting impact on the histogram. When r is zero, φ_r^{AB} responds equally to changes in the closest parts and in the farthest parts of A and B. When $r<0$, it responds more to changes in the farthest parts, and the greater $|r|$ the more asymmetric the response. When $r>0$, it responds more to changes in the closest parts; so much so that the histogram values are infinite if, e.g., $r\geq 1$ and the objects overlap (i.e., the interior of their intersection is not empty). Finally, note that the relative position descriptor φ_r^{AB} becomes a powerful shape descript-

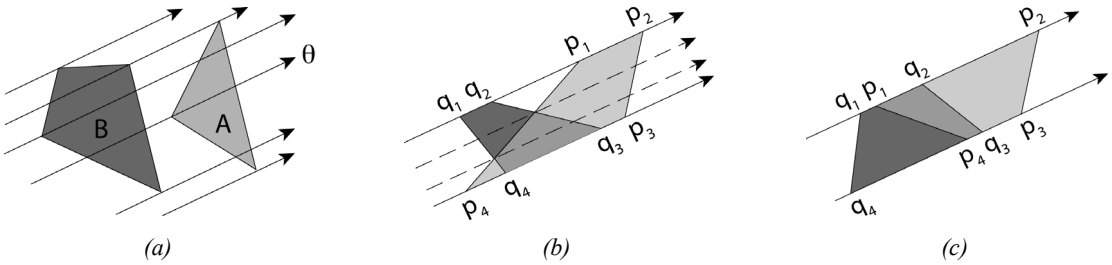

(a) (b) (c)

Figure 2: Partitioning of the objects. *(a)* Each object is divided into trapezoidal pieces. Note that A and B are not necessarily convex or disjoint: there may be more than two pieces between two consecutive lines, and some pieces may intersect. *(b)* The trapezoids $p_1 p_2 p_3 p_4$ and $q_1 q_2 q_3 q_4$ are cut along the dotted lines into three pieces each. *(c)* $p_1 p_2 p_3 p_4$ is broken into $p_1 q_2 q_3 p_4$ and $q_2 p_2 p_3 q_3$, and $q_1 q_2 q_3 q_4$ is broken into $q_1 p_1 p_4 q_4$ and $p_1 q_2 q_3 p_4$.

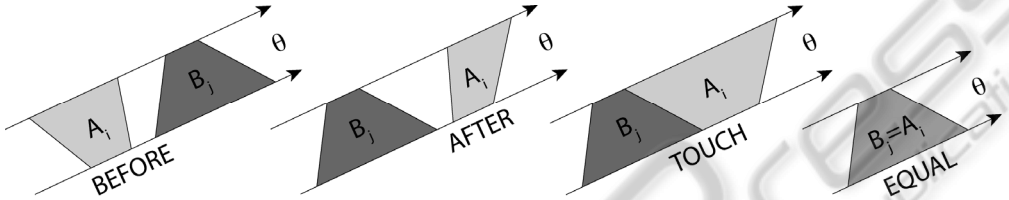

(a) (b) (c) (d)

Figure 3: Two trapezoids A_i and B_j between two consecutive lines. There are 4 cases. Note that in *(a)*, the trapezoids may share one vertex or one edge; in *(b)* they may only share one vertex.

tor when $r<1$ and the two objects A and B are equal (Matsakis et al., 2011).

3 ALGORITHM

3.1 Vector Objects

In the remainder of this paper, we assume that every α_i-cut of an object can be expressed using the union and difference set operations in terms of a finite number of simple polygons P_1^i, P_2^i, P_3^i, …, where the edges of P_u^i and P_v^i do not intersect if $u \neq v$. Note that an object may be crisp or fuzzy, convex or concave, connected or disconnected, and may have holes in it. Practically, each object is described in a text file as the list of its cuts (sorted by increasing α_i); each cut is described as a set of polygons (in any order); each polygon as a list of vertices (listed either clockwise or counterclockwise); each vertex as a pair of coordinates x and y.

3.2 Handling of Vector Objects

As per (7) and (8), the handling of any two objects comes down to the handling of crisp objects. Let us explain, therefore, how to calculate $\varphi_r^{AB}(\theta)$ when A and B are crisp. First, a partition (A_i) of A and a partition (B_j) of B are obtained as follows. The straight lines in direction θ that pass through the objects' vertices divide the objects into trapezoidal (or triangular) pieces (Fig. 2*a*). Consider a piece of A and a piece of B between two consecutive lines. If two nonparallel edges of these pieces intersect, an additional line in direction θ is drawn through the intersection point. This line divides the two pieces into smaller pieces (Fig. 2*b*). Consider two of these smaller pieces, between two consecutive lines. If an edge of the piece of A runs inside the piece of B, or vice versa, both pieces are broken into even smaller pieces (Fig. 2*c*). The partitioning is then complete, and $\varphi_r^{AB}(\theta)$ can be calculated as in (9). Note that $\varphi_r^{A_i B_j}(\theta) = 0$ unless A_i and B_j are between two consecutive lines. If they are, 4 cases must be considered (Fig. 3): in each case, $\varphi_r^{A_i B_j}(\theta)$ can be expressed in terms of r, θ, ε, x_1, x_2, y_1, y_2, z_1, z_2, where x_1, x_2, z_1, z_2 are edge lengths and ε, y_1, y_2 are distances between edges (Fig. 4). These expressions result from the calculation of triple integrals, and are given in Table 2. The functions f_1, f_2, f_3, f_4 are as in Table 1, and $t(\theta) = \max\{|\cos(\theta)|, |\sin(\theta)|\}$.

4 EXPERIMENTS

The general algorithm for force histogram calculation

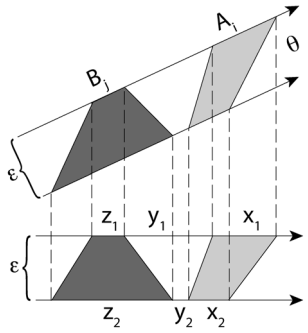

Figure 4: $\varphi_r^{A_iB_j}(\theta)$ can be expressed in terms of r, θ, ε, x_1, x_2, y_1, y_2, z_1, z_2. See Table 2. Note that the vertices of A_i and B_j are projected onto horizontal lines if $|\cos(\theta)| > |\sin(\theta)|$ and onto vertical lines otherwise.

Table 1: The functions f_1, f_2, f_3, f_4.

	$f_1(x,y)$	$f_2(x,y)$	$f_3(x,y)$	$f_4(x,y)$
$x \neq y$	$\frac{y^2(\ln(y)-0.5)-x^2(\ln(x)-0.5)}{y-x}$	$\frac{y\ln(y)-x\ln(x)}{y-x}$	$\frac{\ln(y)-\ln(x)}{y-x}$	$\frac{y^{3-r}-x^{3-r}}{y-x}$
$x=y$	$x\ln(x)$	$1+\ln(x)$	$1/x$	$(3-r)\,x^{2-r}$

Table 2: Expressions for $\varphi_r^{A_iB_j}(\theta)$. See Table 1 and Figs. 3-4.

BEFORE		0
AFTER	$r=0$	$\frac{\varepsilon}{6\,t(\theta)^2}[(x_1+x_2)(z_1+z_2)+x_1z_1+x_2z_2]$
	$r=1$	$\frac{\varepsilon}{2\,t(\theta)}[f_1(x_1+y_1+z_1, x_2+y_2+z_2)+f_1(y_1, y_2)-f_1(x_1+y_1, x_2+y_2)-f_1(y_1+z_1, y_2+z_2)]$
	$r=2$	$-\varepsilon\,[f_2(x_1+y_1+z_1, x_2+y_2+z_2)+f_2(y_1, y_2)-f_2(x_1+y_1, x_2+y_2)-f_2(y_1+z_1, y_2+z_2)]$
	$r=3$	$\frac{\varepsilon\,t(\theta)}{2}[\,f_3(x_1+y_1+z_1, x_2+y_2+z_2)+f_3(y_1, y_2)-f_3(x_1+y_1, x_2+y_2)-f_3(y_1+z_1, y_2+z_2)]$
	else	$\frac{\varepsilon\,[f_4(x_1+y_1+z_1, x_2+y_2+z_2)+f_4(y_1, y_2)-f_4(x_1+y_1, x_2+y_2)-f_4(y_1+z_1, y_2+z_2)]}{t(\theta)^{2-r}(1-r)(2-r)(3-r)}$
TOUCH	$r=1$	$\frac{\varepsilon}{2\,t(\theta)}[f_1(x_1+z_1, x_2+z_2)-f_1(x_1, x_2)-f_1(z_1, z_2)]$
	$r<1$ or $1<r<2$	$\frac{\varepsilon}{t(\theta)^{2-r}(1-r)(2-r)(3-r)}[f_3(x_1+z_1, x_2+z_2)-f_3(x_1, x_2)-f_3(z_1, z_2)]$
	else	$+\infty$
EQUAL	$r<1$	$\frac{\varepsilon}{t(\theta)^{2-r}(1-r)(2-r)(3-r)}f_4(x_1, x_2)$
	else	$+\infty$

in the case of 2-D vector objects was implemented in C, and the experiments were conducted on a Mac OS X 10.6, Intel Core 2 Duo, 2.4 GHz, 4 GB. If the forces are as in (2), then (7) applies, and the algorithm runs in $O(Kk^2 \eta \log \eta)$ time, where K is the number of directions in which forces are considered, k is the number of nonzero membership degrees (k=1 for crisp objects), and η is the total number of object vertices. If the forces are as in (3), then (8) applies, and the algorithm runs in $O(Kk \eta \log \eta)$. The $\eta \log \eta$ part comes from the fact that for every direction θ considered, the partitioning of the objects is achieved by sorting the vertices following direction $\theta+\pi/2$. Figures 5 and 6 show examples of objects and related force histograms, and Fig. 7 shows the processing times of crisp objects in a best case scenario *(a)(b)(c)* and in a worst case scenario *(d)(e)(f)*. Note, *(a)(d)*, that the processing time is minimum when $r = 0$, maximum when r is not an integer (all non-integer r values give about the same processing times), and between these two extremes when r is a nonzero integer. Times to process objects in vector vs. raster forms are compared in *(b)(c)(e)(f)*. For example, *(e)*, calculating the histogram of constant forces ($r = 0$) between two intersecting stars with 50 vertices each (i.e., 25-pointed stars) is about 20 times faster if the stars are in vector form (than if they are in raster form and made of 250K pixels each; whatever the raster algorithm used). Note that for every r and every pair of objects considered in these experiments, the histograms produced by the vector and raster algorithms are visually indistinguishable, and their similarity (as measured by the Tanimoto index) is greater than 99.6%.

5 CONCLUSIONS

A relative position descriptor like the histogram of forces which is endowed with remarkable properties and able to handle any pair of 2-D objects (whether these objects are crisp or fuzzy, connected or disconnected, with or without holes, disjoint or overlapping) is undoubtedly a most useful tool: relative position descriptors are a natural complement to colour, texture, and shape descriptors; the spatial organization of 2-D objects is a subject of interest in many disciplines; spatial regions are modelled by fuzzy sets in an increasing number of applications and areas; examples of regions with holes or multiple connected components abound; examples of regions that touch or overlap abound as well (in particular, fuzzy regions often naturally overlap).

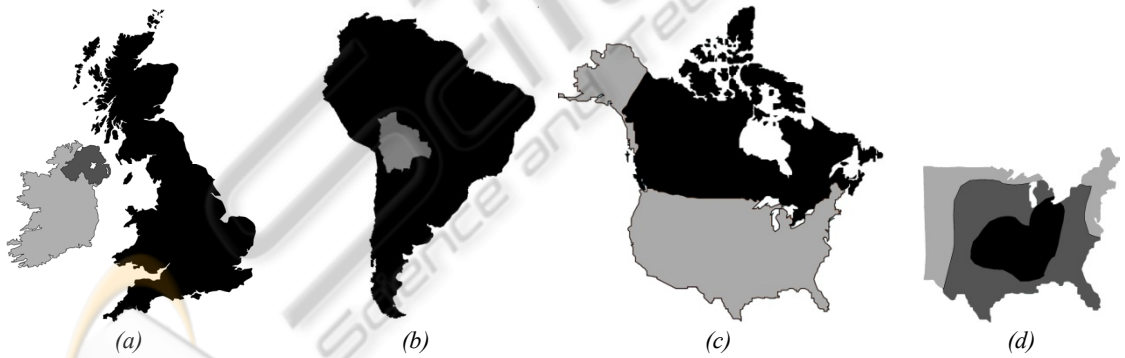

Figure 5: *(a)* Britain and Ireland share Northern Ireland. *(b)* Bolivia in South America. *(c)* Canada and the U.S. *(d)* The risk for strong or violent tornadoes in the U.S. is high (black), medium (dark gray), low (light gray), negligible (elsewhere).

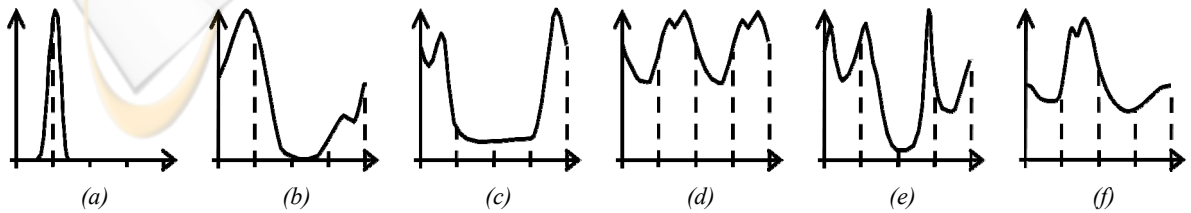

Figure 6: Examples of force histograms. In *(a)*, the objects are disjoint (Canada relative to South America). In *(b)*, they touch (Canada relative to the U.S.). In *(c)*, they overlap (Britain relative to Ireland). In *(d)*, they are equal (the U.S.). In *(e)*, one includes the other (South America and Bolivia). In *(f)*, one is crisp (the U.S.) and the other is fuzzy (tornado risk map).

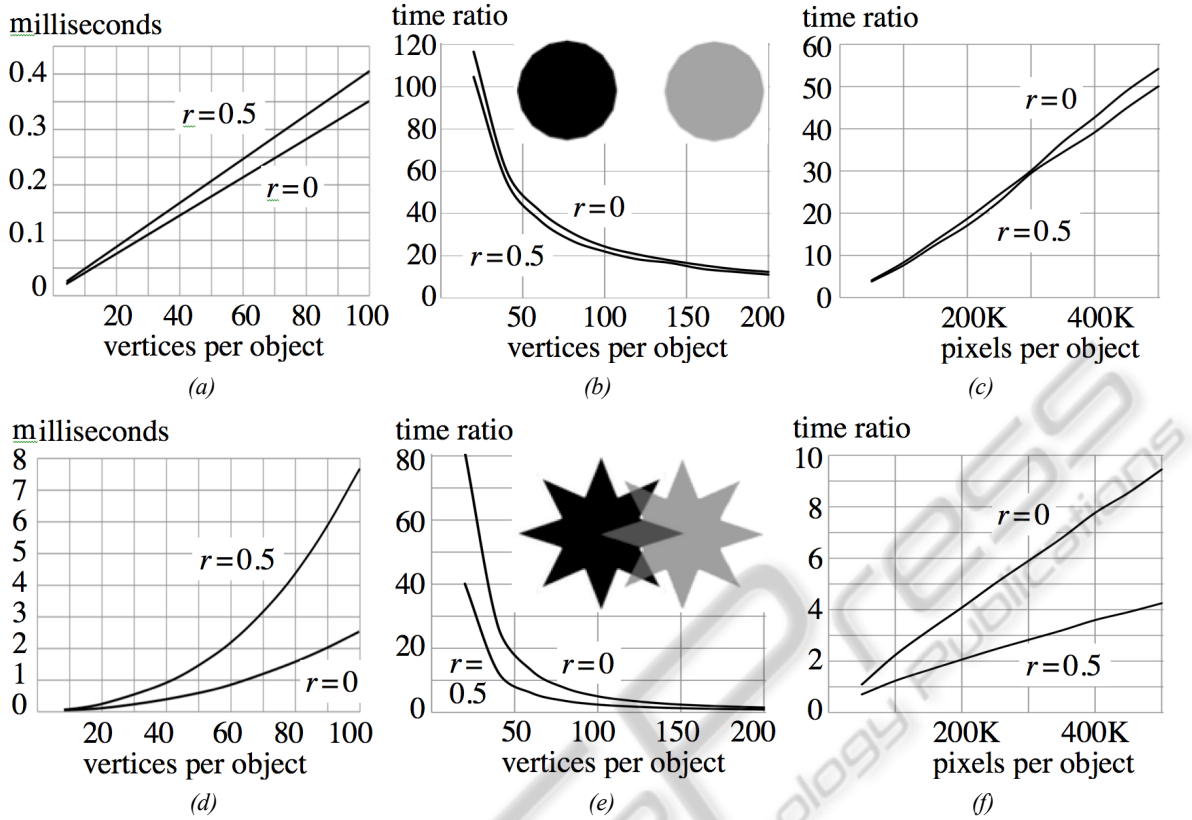

Figure 7: Processing times; in each case, forces were computed in 100 evenly distributed directions. In *(a)(b)(c)*, the objects are crisp disjoint regular convex polygons; in *(d)(e)(f)*, they are crisp intersecting star polygons. In *(a)(d)*, the objects are in vector form and the processing time is the average processing time per direction; note that in *(a)*, only the directions with nonzero forces were actually considered. In *(b)(c)(e)(f)*, the time ratio is the time to process the two objects in raster form divided by the time to process the same two objects in vector form. In *(b)(e)*, each raster object is made of 250K pixels; in *(c)(f)*, each vector object has 100 vertices.

Until now, however, only objects in raster form could be considered. In this paper, we have widened the scope of the histogram of forces to objects in vector form. Since polygons are a fundamental type of data in, e.g., computer graphics and GIS, and are also often used to approximate boundaries of raster regions, this is a significant achievement which should draw the interest of practitioners. Note that all the programs for force histogram computation are freely available upon request. We are currently developing efficient general algorithms for the handling of 3-D raster and vector objects.

ACKNOWLEDGEMENTS

The authors want to express their gratitude for support from the Natural Science and Engineering Research Council of Canada (NSERC), grant 262117.

REFERENCES

Matsakis, P., Wendling, L., 1999. A New Way to Represent the Relative Position of Areal Objects. In *IEEE Trans. on Pattern Analysis and Machine Intelligence*, 21(7), 634-643.

Matsakis, P., Wendling, L., Ni, J., 2011. A General Approach to the Fuzzy Modeling of Spatial Relationships. In Jeansoulin, R., Papini, O., Prade, H., Schockaert, S. (Eds.): *Methods for Handling Imperfect Spatial Information*, Springer-Verlag, 49-74.

Ni, J., Matsakis, P., 2010. An Equivalent Definition of the Histogram of Forces: Theoretical and Algorithmic Implications. In *Pattern Recognition*, 43(4), 1607-1617.

Shyu, C. R., Klaric, M., Scott, G. J., Barb, A. S., Davis, C. H., Palaniappan, K., 2007. GeoIRIS: Geospatial Information Retrieval and Indexing System—Content Mining, Semantics Modeling, and Complex Queries. In *IEEE Trans. on Geoscience and Remote Sensing*, 45(4), 839-852.

Sjahputera, O., Keller, J. M., 2007. Scene Matching Using F-Histogram-Based Features with Possibilistic C-

Means Optimization. In *Fuzzy Sets and Systems*, 158(3), 253-269.

Skubic, M., Perzanowski, D., Blisard, S., Schultz, A., Adams, W., Bugajska, M., Brock, D., 2004. Spatial Language for Human-Robot Dialogs. In *IEEE Trans. on Systems, Man, and Cybernetics Part C*, 34(2), 154-167.

Vaduva, C., Faur, D., Gavat, I., 2010. Data Mining and Spatial Reasoning for Satellite Image Characterization. In *Proceedings of the 8th Int. Conf. on Communications (COMM)*, 173-176.

Wang, Y., Makedon, F., Drysdale, R. L., 2004. Fast Algorithms to Compute the Force Histogram. Pattern Recognition.